

## ELECTRICAL RESISTIVITY VARIATIONS AND PRECIPITATION PROCESSES IN Al-Mg-(Mn)-Cu TYPE ALLOY SHEETS

S. Stanojević, M. Popović, E. Romhanji

Department of Metallurgical Engineering, Faculty of Technology and Metallurgy  
Karnegijeva 4, POB 35-03, 11 120 Belgrade  
Serbia

### ABSTRACT

Precipitation/dissolution processes were followed by electrical resistivity variations in three Al-Mg-(Mn)-Cu alloy sheets: (I) Al-Mg4.5-Mn0.65-Cu0.35, (II) Al-Mg4.2-Mn0.52-Cu0.48, and (III) Al-Mg4.7-Cu0.36, after different thermo-mechanical treatments (TMTs). It was found that precipitation occurs more intensive after solution treatment and cold rolling (535°C/1h+60%) than after the recrystallization annealing and cold rolling (350°C/3h+60%), as the ageing potential in the later procedure was employed in the stage of inter-annealing at 350 °C. Thus, the dissolution processes were dominating in the structure of samples inter-annealed at 350°C and its intensity depends on the Cu content, i.e. the amount of Cu-based particles (S type phase). The contribution in resistivity induced by cold deformation was the most intensive at the beginning of deformation, and it was not influenced by the chemical composition of tested alloys. The resistivity variation with the cold deformation was modeled by power - law equations.

**Keywords:** Al-Mg-(Mn)-Cu alloys; precipitation; resistivity;

### 1. INTRODUCTION

The application of Al-Mg alloy sheets in car body and marine constructions [1,2], becomes very attractive due to their high strength level, good corrosion resistance and a high potential of weight saving. A disadvantage in using Al-Mg alloy sheets in these constructions is that they exhibit softening during the paint-bake sequence [3,4], at temperatures usually ranged from 160° to 180 °C. In case of heat-treatable Al-alloys this problem has been overcome by precipitation hardening at baking temperatures. Following the same idea, it was found that a small addition of Cu in the Al-Mg alloys provides a similar precipitation hardening during paint-bake cycle [5-10]. Such a "hybrid" Al-Mg alloy with a low Cu/Mg ratio: 0.1-0.14 in wt.%, designated as AA5030 [2,11], was supposed to provide much higher strength after paint baking. Earlier was found [12,13] that the precipitation/dissolution processes in Al-alloys can be followed by the electrical resistivity change. The aim of this paper was the using of resistivity measurements for monitoring the precipitation processes in Al-Mg-(Mn)-Cu alloy sheets (with different Cu/Mg and Mn/Mg ratios), which occurs under different thermo-mechanical treatments (TMTs).

### 2. EXPERIMENTAL

**Material.** Two ingots of Al-Mg-Mn-Cu type alloy (*alloys I and II*) were produced by laboratory casting. In respect to the chemical composition which is given in Table 1, they were designated as Al-Mg4.5-Mn0.65-Cu0.35 (*alloy I*) and Al-Mg4.2-Mn0.52-Cu0.48 (*alloy II*) alloys.

Table 1. Chemical composition of the tested Al-Mg-(Mn)-Cu alloys, in wt.%

	Si	Fe	Cu	Mn	Mg	Cr	Ni	Zn	Ti	Be
<i>Alloy I</i>	0,09	0,28	0,35	0,65	4,48	0,096	0,0017	0,031	0,116	0,0032
<i>Alloy II</i>	0,13	0,31	0,48	0,52	4,21	0,136	0,003	0,069	0,010	0,0012
<i>Alloy III</i>	0,13	0,35	0,36	0,05	4,66	0,013	0,003	0,043	0,007	0,00006

The third alloy used in this study Al-Mg4.7-Cu0.36 type (*alloy III*), with no manganese ( $Mn < 0.5\%$ ), was supplied in the cold rolled condition from Impol-Seval Aluminum Rolling Mill. The Cu/Mg ratios were 0.078 and 0.077 for *alloys I and III*, and 0.11 for *alloy II*, while the Mn/Mg ratios were 0.145, 0.123 and 0.011 for the *alloys I, II and III*, respectively.

Two laboratory produced ingots (*alloys I and II*) were homogenized at  $440^{\circ}\text{C}/8\text{h} + 510^{\circ}\text{C}/14\text{h}$ , cooled down to  $470^{\circ}\text{C}/2\text{h}$ , and hot rolled to the thickness of 8 mm. Hot rolled sheets were additionally annealed at  $470^{\circ}\text{C}/1\text{h}$ , in order to ensure fully recrystallized structure, and then cold rolled to 1 mm, with inter-annealing at  $350^{\circ}\text{C}/3\text{h}$ . The industrially produced Al-Mg4.7-Cu0.36 alloy sheets (*alloy III*) were cold rolled to 1 mm, with inter-annealing at  $350^{\circ}\text{C}/3\text{h}$ . All the tested material was further treated in the following manner: (1) *alloys I, II and III* were annealed at  $350^{\circ}\text{C}/3\text{h}$ , cold rolled with 40-60 % reduction, and finally annealed at temperatures from  $220^{\circ}$  to  $470^{\circ}\text{C}/3\text{h}$ ; at  $520^{\circ}$  and  $550^{\circ}\text{C}/10\text{min}$ ; (2) *alloys II and III* were solution treated at  $535^{\circ}\text{C}/1\text{h}$  or annealed at  $320^{\circ}/350^{\circ}\text{C}/3\text{h}$ , cold rolled with 60% reduction, and finally annealed at temperatures from  $220^{\circ}$  to  $470^{\circ}\text{C}/3\text{h}$ .

Electrical resistivity measurements were performed using Sigma test D2.068 equipment ( $f=240\text{ kHz}$ ).

### 3. RESULTS

#### 3.1 Electrical resistivity variations with different TMTs

The electrical resistivity change with final annealing temperatures for the tested alloys II and III, after solution treatment at  $535^{\circ}\text{C}$  or annealing at  $320^{\circ}/350^{\circ}\text{C}$  and 60% cold rolling, has shown in Fig. 1. It can be seen that the cold rolling of solution treated samples ( $535^{\circ}\text{C} + 60\%$ ) brought a significant increase in resistivity, as compared to the samples inter-annealed at  $320^{\circ}/350^{\circ}\text{C}$  and 60% cold rolled.

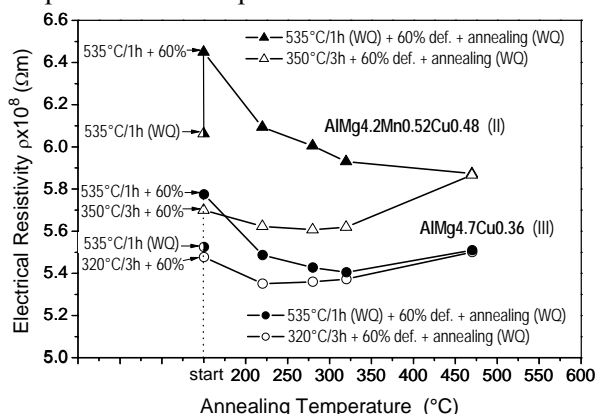


Figure 1. Resistivity variations with annealing temperature for alloys II and III after recrystallization annealing and cold rolling (open symbols) or solution treatment and cold rolling (closed symbols).

Generally, the resistivity level for solution treated samples (*closed symbols*) is much higher than for the samples inter-annealed at  $320^{\circ}/350^{\circ}\text{C}$  (*open symbols*). Fig. 1 has shown that the resistivity of solution treated samples ( $535^{\circ}\text{C}+60\%$ ) decreases rapidly with increasing the annealing temperature, but slightly decreases for inter-annealed samples. After final annealing at higher temperatures ( $> 320^{\circ}\text{C}$ ), the resistivity increases gradually for both alloys, while for alloy II (solution treated, Mn-containing alloy), a continuous decrease in resistivity up to  $470^{\circ}\text{C}$  was observed. It is obvious that the difference between resistivity levels for solution treated (*closed symbols*) and inter-annealed samples (*open symbols*) is more pronounced in case of alloy II (Mn containing), but it diminishes as the temperature of final annealing increases and attains the same level at  $470^{\circ}\text{C}$  for both alloys.

The comparison in resistivity variations with final annealing temperatures for all the tested alloys, after inter-annealing at  $350^{\circ}\text{C}$ , has shown in Fig. 2. The resistivity level is higher for alloys I and II (Mn- and Cu-containing alloys) than for alloy III with no Mn, in the whole range of temperatures. The resistivity changes in respect to the annealing temperatures are rather similar for all the tested alloys: after low temperature annealing (up to  $270^{\circ}\text{C}$ ) the resistivity slightly increases up to the maximum values. An increase in resistivity was found somewhat faster for alloy II with the highest Cu-content. The temperature of maximum resistivity is higher for Mn-containing alloys (alloys I and II) than for

alloy III with no Mn (520°C as compared to 450°C). Maximum resistivity values were unaffected with further increase in temperature up to 550°C, for alloys I and III, but it was decreased for alloy II.

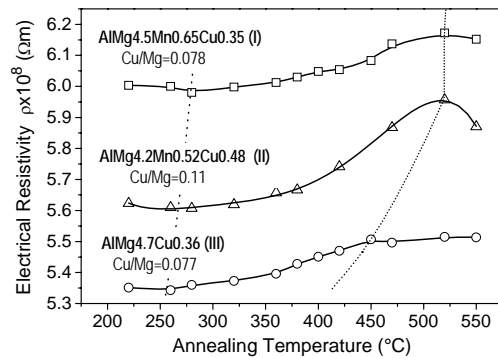


Figure 2. Influence of the final annealing temperature on the resistivity level of all the tested alloys I, II and III, after recrystallization annealing (350°C/3h) and cold rolling (40 – 60 %).

### 3.2 Electrical resistivity variations with cold deformation

Fig. 3a has shown the effect of cold deformation on the resistivity level of alloys II and III. An increase in resistivity by cold rolling, attained the maximum change of  $\sim 0.3 \times 10^{-8} \Omega m$  after the deformation of  $\epsilon=0.9$  for both alloys. The experimental  $\rho-\epsilon$  curves were described by power-law equations and similar parameters were obtained (Fig. 3a). Derivation of the fitted  $\rho-\epsilon$  curves (Fig. 3b) clearly indicates that the contribution of cold deformation in the resistivity level is the highest at the beginning of the cold rolling, while its contribution decreases rapidly at higher deformation.

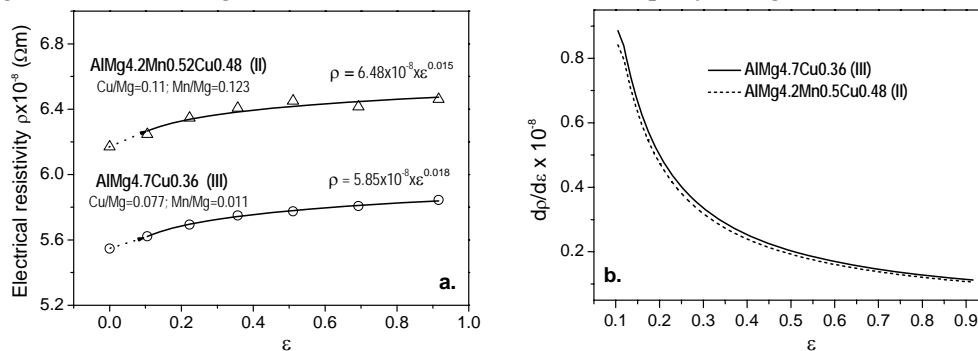


Figure 3. (a) The electrical resistivity variations with cold deformation for alloys II and III, and parameters of the best fit by power-law equations; (b) Derivatives of the fitted  $\rho-\epsilon$  curves.

## 4. DISCUSSION

Precipitation/dissolution processes in Al-Mg-Cu alloys monitored earlier by DSC [8], could be summarized as follows: (1) GPB precipitation (Cu/Mg clusters): at 125°-140°C; (2) GPB dissolution: at 200°-270°C; (3) S'' precipitation ( $Al_2CuMg$ ): at 150°-210°C; (4) S' (S) precipitation ( $Al_2CuMg$  with changed lattice parameters): at 280°-350°C; (5) S' (S) dissolution: at 360°-430°C. It was also recognized [8,9] that the precipitation occurs through two concurrent processes: (i) heterogeneous precipitation at dislocations:  $\alpha \rightarrow S'' \rightarrow S' (S)$ ; and (ii) homogeneous precipitation in the matrix:  $\alpha \rightarrow Cu/Mg$  clusters (GPB zone)  $\rightarrow S'' \rightarrow S' (S)$ .

The resistivity level of the tested alloys II and III was much higher after solution treatment than after inter-annealing at 350°C (Fig. 1), as the alloying elements (Mg, Mn, Cu) were mainly dissolved in the solid solution at 535°C. After annealing at 320°/350°C they were already precipitated as Mn- and Cu-based particles. The additional increase in resistivity brought by cold rolling (Fig. 1) was assumed to be due to an increase of the dislocation density and vacancies concentration, as was stated elsewhere [14]. The deformation induced formation of dislocations and vacancies was found rather saturating by increasing the deformation (Fig. 3), i.e. the majority of them seem to be formed at the beginning of cold rolling. In subsequent annealing of solution treated and cold rolled samples (530°C+60%) up to 320°C, the vacancies have been annealed out, and different types of Cu-based precipitates have been formed (such as GPB, S'', S', S particles), and the resistivity decrease was observed (Fig. 1). It was

assumed that present dislocations and vacancies can aid the diffusion/ precipitation processes [13], which results in a more intensive resistivity drop during annealing of cold rolled than the solution treated samples (Fig. 1). With further increase of the annealing temperature up to 470°C, the resistivity of alloy III (with no Mn) slightly increases probably due to the S'(S) dissolution (Fig. 1, closed circles), while in alloy II (with Mn) the resistivity continuously decreases (Fig. 1, closed triangles). Such a behavior was supposed to be due to the precipitation of Mn-bearing particles [13,15], as they had been partly dissolved during solution treatment at 535°C. The difference between resistivity levels for solution treated (*closed symbols*) and inter-annealed samples (*open symbols*) is more pronounced in case of alloy II because it contains Mn (0.52 wt%) and higher content of Cu (0.48 wt% as compared to 0.36 wt%), as shown in Fig. 1. The contribution of alloying elements in the resistivity is much higher if Mn and Cu are present in the solid solution, than out of solution [12,13]. Thus, the resistivity variation with final annealing is at lower level for the samples with previously precipitated Mn- and Cu- particles (inter-annealed at 350°C) than for the samples with Mn- and Cu- solute in solid solution (solution treated at 535°C). The detailed insight in the resistivity variations with the final annealing given in Fig. 2 revealed that the precipitation processes completed during inter-annealing at 350°C were not affected by further annealing in the low temperature region up to ~ 270°C (min resistivity marked by dashed line in Fig. 2), as those particles stay stable during subsequent annealing. At higher temperatures > 270°C the dissolution processes were dominating in the structure as the resistivity was increased more or less slightly (Fig. 2). The resistivity change with final annealing temperatures indicates that the dissolution processes depend on the chemical composition, and it was the most intensive in the alloy II with the highest Cu-content, i.e. highest content of Cu-based particles (Fig. 2). It is also worth noting that general resistivity level for the Mn-containing alloys (alloys I and II) is higher than for the alloy III with no Mn (Fig. 2), due to the Mn contribution in resistivity level. However, the highest resistivity level for alloy I can be attributed to higher Mn-content than in alloy II, and to the presence of other alloying elements, such as Ti (Table 1), which significantly affect the resistivity level [12,13].

## 5. SUMMARY

Precipitation/dissolution processes were followed by electrical resistivity variations in the Al-Mg-(Mn)-Cu alloy sheets: (I) Al-Mg4.5-Mn0.65-Cu0.35 ( $Cu/Mg=0.078$ ,  $Mn/Mg=0.145$ ), (II) Al-Mg4.2-Mn0.52-Cu0.48 ( $Cu/Mg=0.11$ ,  $Mn/Mg=0.123$ ) and (III) Al-Mg4.7-Cu0.36 ( $Cu/Mg=0.077$ ,  $Mn/Mg=0.011$ ), after different thermo-mechanical treatments (TMTs). It was found that precipitation occurs more intensive after solution treatment and cold rolling (535°C/1h+60%) than after the recrystallization annealing and cold rolling (350°C/3h+60%), as the ageing potential in the later procedure was employed in the stage of inter-annealing at 350°C. Thus, the dissolution processes were dominating in the structure of samples inter-annealed at 350°C, and its intensity depends on the Cu content, i.e. the amount of Cu-based particles (S type phase). The increase in resistivity induced by cold deformation was the most intensive at the beginning of deformation, and not influenced by the chemical composition of tested alloys.

## 6. REFERENCES

- [1] R.E. Sanders Jr., P.A. Hollinshead, E.A. Simielli, *Materials Forum*, **28** (2004) 53-64
- [2] K. Kobayashi, S. Koga, M. Hino, *Conf. Proc. 1<sup>st</sup> Japan International SAMPE Symposium*, (1989) 59-64
- [3] G.B. Burger, A.K. Gupta, P.W. Jeffrey, D.J. Lloyd, *Mater. Characterization*, **35** (1995) 23
- [4] J. Hirsch, *Mater. Sci. Forum*, **242** (1997) 33
- [5] T. Fujita, K. Hasegawa, M. Saga: *European Patent No.0616044 A2* (1994).
- [6] Y. Suzuki, M. Matsuo, M. Saga, M. Kikuchi, *Mater. Sci. Forum*, vols. **217-222** (1996) 1789
- [7] P. Ratchev, B. Verlinden, P. De Smet, P. Van Houtte, *Materials Trans., JIM*, No1, **40** (1999) 34
- [8] P. Ratchev, B. Verlinden, P. De Smet, P. Van Houtte, *Acta mater.*, **46** (1998) 3523
- [9] P. Ratchev, B. Verlinden, et al., in *Proc of ICAA-6: Aluminum Alloys*, vol.2, 1998, p.757
- [10] B. Verlinden, P. Ratchev, et al., in *Proc of ICAA-6: Aluminum Alloys*, vol.2, 1998, p.1075
- [11] J.M. Story, G.W. Jarvis, H.R. Zonker, S.J. Murtha, *SAE Paper No.930277* (1993) 320
- [12] J.F. Hatch, *Aluminium: Properties and Physical Metallurgy*, ASM, Metals Park Ohio, 1984.
- [13] S.I. Vooijs, S.B. Davenport, I. Todd, S. van der Zwaag, *Philosophical Mag.*, **A81** (2001) 2059
- [14] W.F. Hosford, "Physical Metallurgy", 2005, Taylor & Francis, p.152
- [15] S. Vooijs, B. Davenport, S. van der Zwaag, In *Proc. of "EOROMEAT99"*, vol 3 (1999) 90-95